Research Article

Korean Red Ginseng suppresses emphysematous lesions induced by cigarette smoke condensate through inhibition of macrophage-driven apoptosis pathways

Jeong-Won Kim, Jin-Hwa Kim, Chang-Yeop Kim, Ji-Soo Jeong, Je-Won Ko [*], Tae-Won Kim [**]

College of Veterinary Medicine (BK21 FOUR Program), Chungnam National University, 99 Daehak-ro, Daejeon, Republic of Korea

ABSTRACT

Background: Cigarette smoke is generally accepted as a major contributor to chronic obstructive pulmonary disease (COPD), which is characterized by emphysematous lesions. In this study, we investigated the protective effects of Korean Red Ginseng (KRG) against cigarette smoke condensate (CSC)-induced emphysema.
Methods: Mice were instilled with 50 mg/kg of CSC intranasally once a week for 4 weeks, KRG was administered to the mice once daily for 4 weeks at doses of 100 or 300 mg/kg, and dexamethasone (DEX, positive control) was administered to the mice once daily for 2 weeks at 3 mg/kg.
Results: KRG markedly decreased the macrophage population in bronchoalveolar lavage fluid and reduced emphysematous lesions in the lung tissues. KRG suppressed CSC-induced apoptosis as revealed by terminal deoxynucleotidyl transferase deoxyuridine triphosphate nick-end labeling staining and Caspase 3 immunohistochemistry. Additionally, KRG effectively inhibited CSC-mediated activation of Bcl-2-associated X protein/Caspase 3 signaling, followed by the induction of cell survival signaling, including vascular endothelial growth factor/phosphoinositide 3-kinase/protein kinase B *in vivo* and *in vitro*. The DEX group also showed similar improved results *in vivo* and *in vitro*.
Conclusion: Taken together, KRG effectively inhibits macrophage-mediated emphysema induced by CSC exposure, possibly via the suppression of pro-apoptotic signaling, which results in cell survival pathway activation. These findings suggest that KRG has therapeutic potential for the prevention of emphysema in COPD patients.

1. Introduction

Chronic obstructive pulmonary disease (COPD) was the third leading cause of death worldwide in 2016 [1]. The incidence of COPD is expected to increase in the future owing to exposure to risk factors for COPD, especially cigarette smoke (CS) [2,3]. Although the symptoms of COPD are varied and complex, emphysema is a characteristic phenotype of this disease [4]. According to recent studies, inflammation, oxidative stress, protease-antiprotease imbalance, and alveolar apoptosis are the four major mechanisms of emphysema that have been established or proposed [5,6]. In these pathogeneses, macrophages are known to play important roles in the clearance of exogenous particles and activation of signal molecules related to the onset of emphysema. Clinical studies have shown that the number of macrophages in the respiratory system is increased in patients with COPD, and that the number of macrophages is closely related to the severity of emphysema [7,8]. Therefore, controlling the macrophage population in the airway is regarded as a therapeutic goal for reducing emphysema in COPD induced by CS exposure.

Korean Red Ginseng (KRG, *Panax ginseng* Meyer), one of most widely used medicinal herbs, has been reported to exert various pharmacological effects in both in vivo and in vitro experiments, including immune-enhancing, anti-inflammation, anti-oxidation, and anti-cancer effects [9–11]. Several studies have reported that KRG and its main components exert protective effects against pulmonary diseases, including acute lung injury, asthma, and COPD [12–14]. In particular, KRG reduces apoptosis in lung cancer and ginsenoside, one of its main active ingredients, attenuates CS-induced epithelial-mesenchymal transition in COPD rats [15,16]. Furthermore, Shergis et al reported that ginsenosides inhibit kinase phosphorylation including MAPK and ERK1/2, NF-κB transcription factor induction/translocation and

decrease pro-inflammatory mediators, TNF-α, IL-6, IL-8, ROS, protease to protect from oxidative stress of COPD [14]. Based on this evidence, we hypothesized that KRG could suppress alveolar emphysema induced by cigarette smoke condensate (CSC) through the inhibition of apoptotic signaling.

Thus, we investigated the effects of KRG on CSC-induced emphysema by measuring the macrophage population and performing a histological analysis. Additionally, we assessed the effects of KRG on apoptotic protein expression and cell survival signaling to elucidate the mechanisms underlying emphysema progression.

2. Materials and methods

2.1. Contents of ginsenoside in KRG

KRG was obtained from the Korea Ginseng Corporation (Daejeon, Republic of Korea), and quality control was performed by confirming the major ginsenoside components, Rb1, Rb2, Rd, Rg1 and Rg3, using high-performance liquid chromatography-ultraviolet, according to our previous study [13]. The Rb1, Rb2, Rd, Rg1, and Rg3 contents in KRG were approximately 6.7, 2.1, 1.0, 1.6, and 1.5 mg/g, respectively (Fig. S1).

2.2. In vivo experiments

2.2.1. Animals and environmental conditions

Specific pathogen-free male C57BL/6N mice (6 weeks old, 20–25 g) were purchased from Orient Bio Co. (Seongnam, Republic of Korea) and quarantined and acclimated for one week before the experiments. All mice were housed under controlled standard conditions (temperature, $23 \pm 3°C$; humidity, $50 \pm 10\%$; 12 h light/dark cycles; 13–18 air changes/h) with water and commercial rodent chow (Samyang Feed, Wonju, Republic of Korea) provided ad libitum. All experiments were approved by the Institutional Animal Care and Use Committee of Chungnam National University and performed in compliance with the Guidelines for Animal Experiments of Chungnam National University (Approval no.202206A-CNU-121; June 29, 2022).

2.2.2. Experimental groups and emphysema mouse model

The animal studies used two different designs. For dose-dependency study, twenty-four healthy male mice were randomly allocated into four groups as follows: (1) NC (normal control, vehicle intranasal instillation + vehicle perorally (p.o.)) group; (2) CSC (CSC intranasal instillation, 50 mg/kg/week + vehicle p.o.) group; (3), (4) CSC + KRG 100 and CSC + KRG 300 (CSC intranasal instillation, 50 mg/kg/week + KRG p.o., 100 or 300 mg/kg/day, respectively) groups ($n = 6$ per group).

For comparative studies with drugs, twenty-four healthy male mice were randomly allocated into four groups as follows: (1) NC (vehicle intranasal instillation + vehicle perorally (p.o.) group; (2) CSC (CSC intranasal instillation, 50 mg/kg/week + vehicle p.o.) group; (3) DEX (CSC intranasal instillation, 50 mg/kg/week + DEX (dexamethasone) p.o., 3 mg/kg/day) (4) CSC + KRG 300 (CSC intranasal instillation, 50 mg/kg/week + KRG p.o., 300 mg/kg/day) groups ($n = 6$ per group). To randomize between groups, all mice were weighed and the groups were distributed so that the average mouse weight in each group was the same.

The CSC was obtained from the Korea Institute of Toxicology (Jeongeup, Republic of Korea). Under anesthesia, the mice were administered CSC 50 mg/kg intranasally once a week for 4 weeks. KRG and DEX were dissolved in phosphate-buffered saline (PBS) and administered to the mice once daily via oral gavage for 4 weeks or 2 weeks, respectively. The effective KRG dose, respiratory toxic CSC dose, and end time point after CSC administration were selected based on the results of our preliminary study and a previous study [17]. The ginsenoside contents in the KRG was determined by HPLC analysis and the 5 uL of KRG was injected into the HPLC for column separation. Based on the sum of major ginsenoside contents we found which was less than

total 10 mg/g, we set the dose range for the animal experiment to 100 and 300 mg/kg. In toxicity study, oral dose of 2000 mg/kg/day was no observed adverse effect level (NOAEL) in SD rats for 13 weeks [18]. Considering these points, doses of 100 and 300 mg/kg/day used in this study are considered reasonable doses to test.

2.2.3. Macrophage count in bronchoalveolar lavage fluid (BALF)

To obtain BALF from mice, the mice were sacrificed by carbon dioxide inhalation 24 h after the last CSC exposure. Tracheostomy and BALF sampling were performed according to previously published methods [19]. Macrophage counts in BALF were determined using Diff-Quik® staining reagent (Sysmex Corporation, Kobe, Japan).

2.2.4. Histopathological examination

A portion of the formalin-fixed lung was processed, embedded in paraffin, and sectioned into 4 μm-thick sections. Sections were deparaffinized and rehydrated using standard techniques and then stained with Harris' hematoxylin and eosin (TissuePro Technology, Gainesville, FL, USA) for microscopic examination (Leica DM LB2; Leica, Wetzlar, Germany). To evaluate emphysematous lesions, fields of view were randomly selected and manually observed using a light microscope with $10 \times$ and $20 \times$ objective lenses and a $100 \times$ oil immersion lens. The mean linear intercept length (MLI) was calculated manually according to previous study [20].

2.2.5. Terminal deoxynucleotidyl transferase deoxyuridine triphosphate nick end labeling TUNEL) and immunohistochemistry (IHC) for the evaluation of Caspase 3 expression

Apoptosis was detected in the lung tissue using a TUNEL assay kit (ApopTag® Peroxidase In Situ Apoptosis Detection Kit; Millipore Corporation, Billerica, MA, USA), according to the manufacturer's instructions. Apoptotic changes were visualized with 3,3-diaminobenzidine (DAB) chromogen and counterstained with Harris hematoxylin before mounting.

Caspase 3 expression was visualized using an IHC kit (Abcam, Cambridge, UK) following the manufacturer's protocol. Anti-Caspase 3 antibody (1:200 dilution; Cell Signaling Technology, Danvers, MA, USA) and goat anti-rabbit immunoglobulin G were used as the primary and secondary antibodies, respectively. The DAB chromogen was counterstained with Harris hematoxylin. Each slide was examined in a blinded manner under a light microscope (Leica). Ten random non-overlapping fields per slide were acquired, and quantitative image analysis was performed using an image analyzer (IMT i-Solution software, Houston, TX, USA).

2.2.6. Immunoblotting

The frozen lung tissue was homogenized (1:9, w/v) with a tissue lysis/extraction reagent (Sigma-Aldrich, St. Louis, MO, USA) containing a protease/phosphatase inhibitor cocktail (Sigma-Aldrich) and was centrifuged at $12,000 \times g$ for 10 min at $4°C$ to isolate the cellular proteins in the supernatant. To investigate the protein expression levels related to apoptotic changes, we performed western blotting according to a previous study [21]. The following primary antibodies and dilutions were used: total phosphatidylinositol 3-kinase (PI3K; 1:1000 dilution; Abcam), phospho (p)-PI3K (1:1000 dilution; Abcam), total protein kinase B (AKT; 1:1000 dilution; Abcam), p-AKT (1:1000 dilution; Abcam), B-cell lymphoma 2 (Bcl-2; 1:1000 dilution; Abcam), Bcl-2-associated X protein (Bax; 1:1000 dilution; Abcam), β-actin (1:2000 dilution; Abcam), vascular endothelial growth factor (VEGF; 1:1000 dilution; Novus Biologicals, Littleton, CO, USA), and cleaved Caspase 3 (1:1000 dilution; Cell Signaling Technology). Relative protein expression levels were determined using Chemi-Doc (Bio-Rad Laboratories, Hercules, CA, USA).

2.3. In vitro experiments

2.3.1. Cell culture and cell viability

The human airway epithelial cell line NCI–H292 was maintained in RPMI 1640 supplemented with 10% fetal bovine serum and penicillin/streptomycin at 37°C in a 5% CO_2 incubator with 95% air. Cell viability in response to CSC and KRG was measured using an EZ-Cytox cell viability assay kit (DoGenBio Co., Ltd., Seoul, Republic of Korea). Briefly, NCI–H292 cells were cultured in 96-well plates at a density of 2.5×10^4 cells/well for 24 h. The cells were subsequently treated with various concentrations of CSC and KRG. After culturing for 24 h, 10 μL of the kit solution was added to each well and incubated for 2 h at 37°C and 5% CO_2. Cell viability was determined by measuring absorbance at 450 nm using an enzyme-linked immunosorbent assay reader (Bio-Rad Laboratories). Cell viability was determined relative to that of the untreated control cells.

2.3.2. Evaluation of mRNA expression levels

Total RNA was isolated using the SmartGene Total RNA Extraction Kit (SJ Bioscience, Daejeon, Republic of Korea), according to the manufacturer's protocol. First-strand cDNA was synthesized using 1 μg of total RNA and the Compact cDNA Synthesis Kit (SJ Bioscience). SYBR Green-based quantitative polymerase chain reaction (PCR) amplification was performed using the CFX™ Connect Real-Time System (Bio-Rad Laboratories) and SYBR Green Q-PCR Master Mix with Low Rox (SJ Bioscience) with first-strand cDNA diluted 1:20 and 10 pmol of each primer, according to the manufacturer's protocols. The following primers were used to amplify human-specific genes: interleukin (IL)-1β forward, 5-AGC CAG GAC AGT CAG CTC TC-3 and reverse, 5-ACT TCT TGC CCC CTT TGA AT-3; IL-6 forward, 5-ATG CAA TAA CCA CCC CTG AC-3, and reverse, 5-ATC TGA GGT GCC CAT GCT AC-3; tumor necrosis factor (TNF)-α forward, 5-CAA AGT AGA CCT GCC CAG AC-3 and reverse, 5-GAC CTC TCT CTA ATC AGC CC-3; and glyceraldehyde 3-phosphate dehydrogenase (GAPDH) forward, 5-GAT TTG GTC GTA TTG GGC GC-3 and reverse, 5-AGT GAT GGC ATG GAC TGT GG-3. The relative quantities of the targets were normalized to that of the endogenous GAPDH control and expressed as $2^{-\Delta\Delta Ct}$ (fold), where ΔCt = Ct of the target gene – Ct of the endogenous control gene and$\Delta\Delta Ct = \Delta Ct$ of the target gene samples – ΔCt of the calibrator for the target gene.

2.3.3. Immunoblotting

The cells were treated with various concentrations of KRG (160, 320, and 640 μg/mL), montelukast sodium (MON, 10μM; Merck & Co., NJ) and DEX (1μM; Sigma, MO) followed by incubation with CSC (100 μg/mL) for the indicated times. The cells were collected by washing twice with PBS and resuspended in RIPA buffer (Sigma–Aldrich) containing a protease/phosphatase inhibitor cocktail (Sigma–Aldrich). Immunoblotting was performed as previously described [21]. The primary antibodies used were as follows: total PI3K (1:1000 dilution; Abcam), p-PI3K (1:1000 dilution; Abcam), total AKT (1:1000 dilution; Abcam), p-AKT (1:1000 dilution; Abcam), Bax (1:1000 dilution; Abcam), β-actin (1:2000 dilution; Abcam), VEGF (1:1000 dilution; Novus Biologicals), and cleaved Caspase 3 (1:1000 dilution; Cell Signaling Technology). Relative protein expression was determined using Chemi-Doc (Bio-Rad Laboratories).

2.4. Statistical analyses

The results are expressed as the mean ± standard deviation, and all statistical comparisons were determined via one-way analysis of variance followed by the post-hoc Tukey's honestly significant difference test. Statistical significance between the treatment groups and NC group was determined using GraphPad InStat v. 3.0 (GraphPad Software, Inc., La Jolla, CA, USA). Statistical significance was set at a *p*-value less than 0.05.

3. Results

3.1. In vivo experiments

3.1.1. Effects of KRG on macrophage counts in BALF

To evaluate the preventive effects of KRG on the alveolar macrophage population in BALF, Diff-Quik® staining was performed. As shown in Fig. 1A, the CSC group had a significantly higher macrophage count in BALF compared with the NC group. In contrast, the KRG (100 and 300 mg/kg)-treated groups showed a marked dose-dependent reduction in the macrophage population in the BALF compared with the CSC group. The macrophage cell counts of the DEX group was significantly decreased than that of the OVA group.

3.1.2. Effect of KRG on emphysematous lesions in CSC-exposed animals

As shown in Fig. 1B, the lung tissue of CSC-exposed animals showed significant emphysematous lesions represented by enlarged air spaces compared with the NC group. However, similar to the DEX group, the emphysematous lesions caused by CSC exposure were attenuated in KRG (100 and 300 mg/kg)-treated animals which revealed by results of MLI.

3.1.3. Effects of KRG on CSC-induced apoptotic changes

To determine whether KRG elicits CSC-induced apoptotic changes, we evaluated apoptosis by TUNEL and Caspase 3 expression levels via IHC. The number of TUNEL-positive cells in the alveoli was higher in the CSC group than that in the NC group (Fig. 2A). In contrast, compared with the CSC group, KRG (100 and 300 mg/kg)-treated groups showed fewer TUNEL-positive cells in a dose-dependent manner. Similarly, compared with the CSC group, the number of Caspase 3-positive cells induced by CSC treatment was reduced in the KRG (100 and 300 mg/kg)-treated groups in a dose-dependent manner (Fig. 2B). These histological changes in the lung were similar to that found in the DEX group.

3.1.4. Effects of KRG on the expression of apoptotic pathway proteins

As shown in Fig. 3A and B, CSC treatment significantly increased Bax expression compared to that in the NC group. In contrast, enhanced Bax expression was markedly suppressed by KRG treatment (100 and 300 mg/kg). Similar results were observed for Caspase 3 expression. The expression levels of Caspase 3 were higher in the CSC group than the NC group, whereas the KRG (100 and 300 mg/kg) groups had significantly reduced Caspase 3 expression levels compared with the CSC group. Regarding the expression levels of Bcl-2, the CSC group showed markedly decreased levels compared with the NC group, while the KRG (100 and 300 mg/kg) groups showed significantly increased levels compared with the CSC group. The protective effects of KRG against CSC showed a dose-response relationship for all proteins related to apoptosis.

3.1.5. Effects of KRG on the expression of cell survival pathway proteins

VEGF expression was significantly higher in the CSC group than that in the NC group (Fig. 3C and D). In contrast, KRG treatment markedly suppressed the upregulation of VEGF expression in a dose-dependent manner. Moreover, PI3K/AKT phosphorylation was consistent with the VEGF expression pattern. The CSC group had a significantly higher level of PI3K/AKT phosphorylation than the NC group; on the other hand, the KRG (100 and 300 mg/kg) groups had a significantly lower level of phosphorylation compared with the CSC group. The effect of KRG on proteins in the cell survival pathway was dose-dependent, and all protein expression levels were statistically significant ($p < 0.01$) in the CSC + KRG 300 group.

3.2. In vitro experiments

3.2.1. Effect of KRG on cell viability and mRNA expression of proinflammatory cytokines in CSC-stimulated H292 cells

CSC and KRG were found to have no cytotoxic effect on H292 cells at concentrations of up to 100 and 640 μg/mL, respectively (Fig. 4A and B).
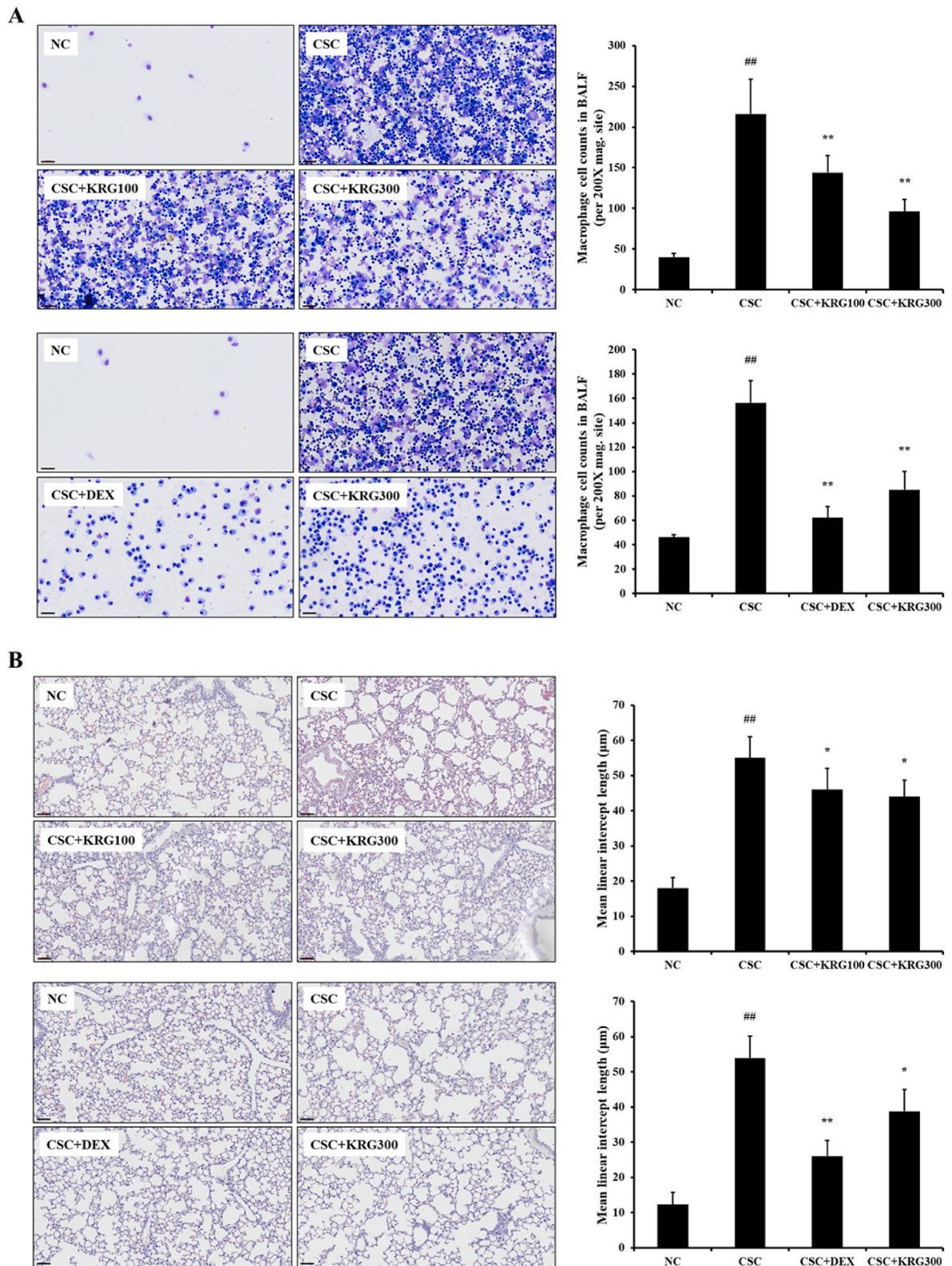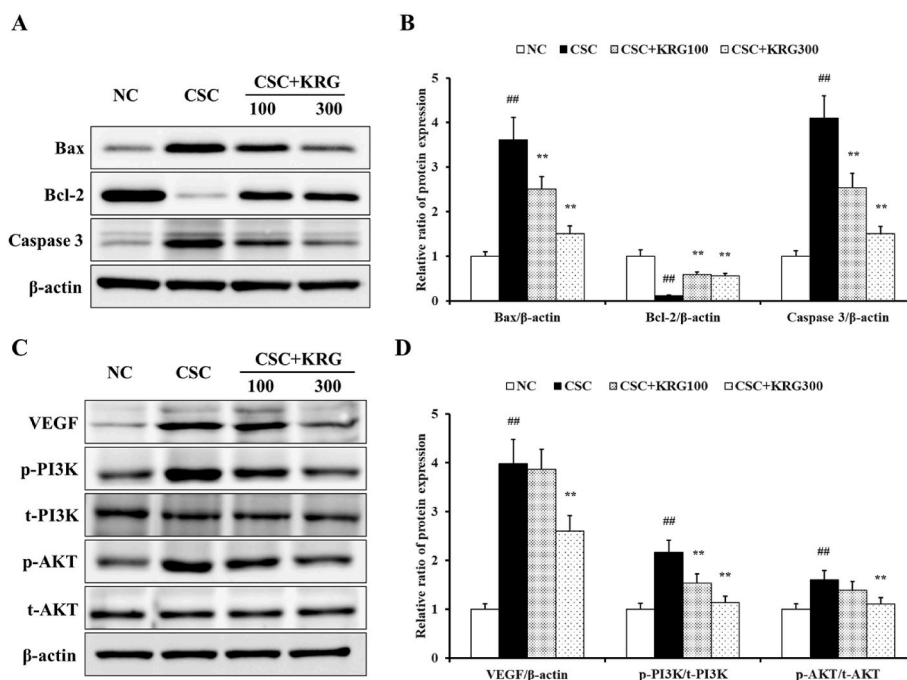
Fig. 1. Korean Red Ginseng (KRG) reduces the elevated (A) macrophage cell counts in bronchoalveolar lavage fluids (BALF) and alleviated the (B) emphysematous lesions in lung tissues. NC; mice instilled with vehicle + vehicle p.o., CSC; mice instilled with cigarette smoke condensate (CSC) + vehicle p.o., CSC + DEX; mice instilled with CSC + DEX 3 mg/kg/day p.o., CSC + KRG100 and CSC + KRG300; mice instilled with CSC + KRG 100 or 300mg/kg/day p.o., respectively. Values: means $\pm$ standard deviation ($n = 6$). Significance: $^{\#\#}p < 0.01$ vs NC; *, **$p < 0.05$ and 0.01 vs CSC, respectively.
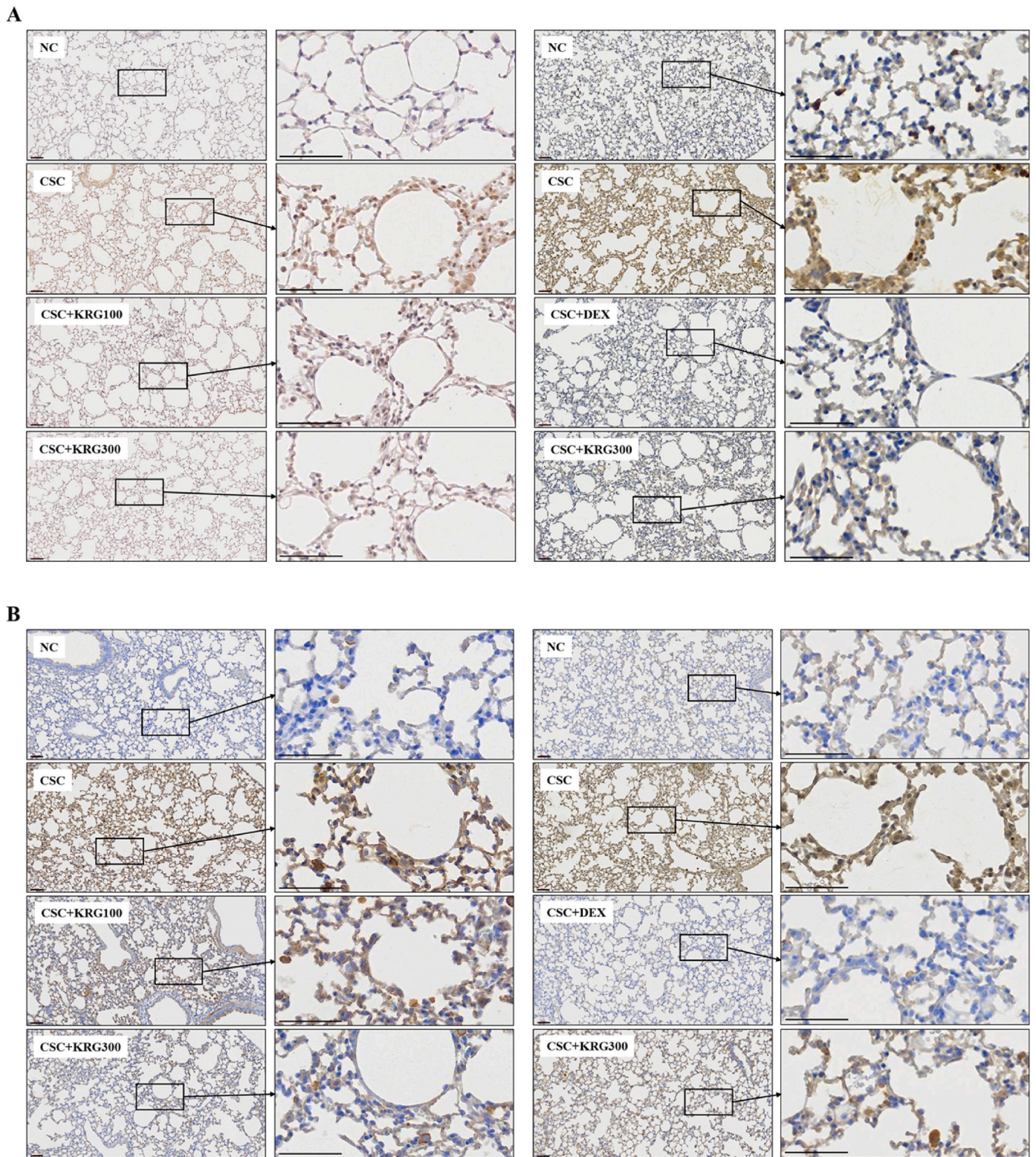
Fig. 2. Korean Red Ginseng (KRG) reduces the elevated (A) Caspase 3 positivity revealed by immunohistochemistry and (B) TUNEL positivity in lung tissues from mice. NC; mice instilled with vehicle + vehicle p.o., CSC; mice instilled with cigarette smoke condensate (CSC) + vehicle p.o., CSC + DEX; mice instilled with CSC + DEX 3 mg/kg/day p.o., CSC + KRG100 and CSC + KRG300; mice instilled with CSC + KRG 100 or 300mg/kg/day p.o., respectively.

Therefore, KRG levels of up to 640 μg/mL were used for subsequent experiments. The CSC-stimulated cells exhibited a significant increase in the mRNA expression levels of IL-1β, IL-6, and TNF-α compared to the untreated cells. However, the CSC-induced mRNA expression levels of proinflammatory cytokines were significantly reduced by KRG treatment in a concentration-dependent manner. Also, the positive controls, MON and DEX, significantly reduced the mRNA levels of proinflammatory cytokines (Fig. 4C–E).

Fig. 3. Korean Red Ginseng (KRG) reduces the (A) expression of Bcl-2-associated X protein (Bax) and Caspase 3, and induced the expression of B-cell lymphoma 2 (Bcl-2), and (C) expression of vascular endothelial growth factor (VEGF) and phosphorylation of phosphatidylinositol 3-kinase (PI3K) and protein kinase B (AKT) in lung tissues, of which (B), (D) densitometric values were determined using Chemi-Doc. NC; mice instilled with vehicle + vehicle p.o., CSC; mice instilled with cigarette smoke condensate (CSC) + vehicle p.o., CSC + DEX; mice instilled with CSC + DEX 3 mg/kg/day p.o., CSC + KRG100 and CSC + KRG300; mice instilled with CSC + KRG 100 or 300mg/kg/day p.o., respectively. Values: means ± standard deviation ($n = 6$). Significance: $^{\#\#}p < 0.01$ vs NC; $^{**}p < 0.01$ vs CSC.

3.2.2. Effects of KRG on the protein expression levels of apoptotic pathway in CSC-stimulated H292 cells

CSC treatment increased Bax expression compared to that in the untreated cells. However, KRG treatment decreased CSC-induced upregulation of Bax expression in a concentration-dependent manner (Fig. 5). Similarly, the CSC-stimulated cells exhibited significantly elevated Caspase 3 expression compared to untreated cells, while the KRG-treated cells showed a noticeable decrease in Caspase 3 expression compared to CSC-stimulated cells. In addition, the positive controls significantly reduced apoptotic protein expression level.

3.2.3. Effects of KRG on the expression levels of cell survival pathway genes in CSC-stimulated H292 cells

CSC-stimulated cells showed increased VEGF expression compared to untreated cells. However, KRG-treated cells exhibited a decrease in VEGF expression levels compared to CSC-stimulated cells in a concentration-dependent manner (Fig. 6). Phosphorylation of PI3K/AKT showed similar results to those observed for VEGF expression. The CSC-stimulated cells exhibited a marked elevation in the phosphorylation of PI3K/AKT compared to untreated cells, whereas the KRG-treated cells exhibited a marked decline in PI3K/AKT phosphorylation compared to CSC-stimulated cells. Also, the MON and DEX notably reduced VEGF and the phosphorylation of PI3K/AKT expression level.

4. Discussion

CS is a major cause of COPD, which is characterized by emphysematous lesions, defined as alveolar destruction and enlargement [22]. Macrophages play a crucial role in the complex pathogenesis of emphysema, especially when airborne hazardous substances, such as CS, are involved [5,6]. To confirm the role of macrophages in emphysema progression more clearly, unlike previous studies, we conducted experiments using CSC, which reflects the particulate phase more than CS. Additionally, we studied the preventive effect of KRG on emphysematous changes in a CSC-induced COPD mouse model and in

CSC-stimulated H292 cells. KRG significantly reduced the macrophage population in BALF and emphysematous lesions induced by CSC instillation. In addition, KRG decreased apoptotic changes in CSC-treated lung tissue and related pro-apoptotic proteins, including Bax and Caspase 3, which resulted in the compensatory elevation of cell survival signaling, such as the VEGF/PI3K/AKT pathways.

Macrophages play critical roles in the development of COPD [23–25]. Pulmonary macrophages are primary innate immune cells that distinguish, swallow, and destroy inhaled particles, including CS and particulate matter, which are the major environmental factors for COPD [26]. In various clinical studies, a large number of macrophages were detected in the BALF, lung, and sputum samples of COPD patients, and the number of macrophages in the parenchyma was quantitatively correlated with the severity of emphysema [8,27,28]. In particular, Finkelstein et al [29] showed an increase in the number of macrophages located at the alveolar wall rupture/emphysema site. These studies demonstrate the potential role of macrophages in the development of emphysema. In this study, KRG treatment markedly reduced the CSC-induced macrophage population in BALF in a dose-dependent manner. The reduction in macrophage count was consistent with the attenuation of emphysematous lesions in lung tissues after CSC instillation with KRG. The symptoms of emphysema, which are proportional to the number of macrophages, suggest that macrophages play an important role in emphysema pathogenesis. Our results also indicate that the ameliorative effect of KRG against emphysema stems from its ability to reduce the macrophage population.

Among the established and proposed mechanisms of the pathogenesis of emphysema, which is a key phenotype of COPD, alveolar apoptosis is a primary contributor to the development of emphysema [6, 22,30]. Macrophages are one of the main sources of endogenous reactive oxygen species (ROS) due to the phagocytosis of inhaled particles [30]. Although the ROS may act directly in pathogen killing, they may also be involved as secondary signaling messengers that induce apoptosis [6]. Apoptosis is a programmed cell death that involves the mitochondrial pathway [31]. It is regulated by the Bcl-2 family of proteins and is
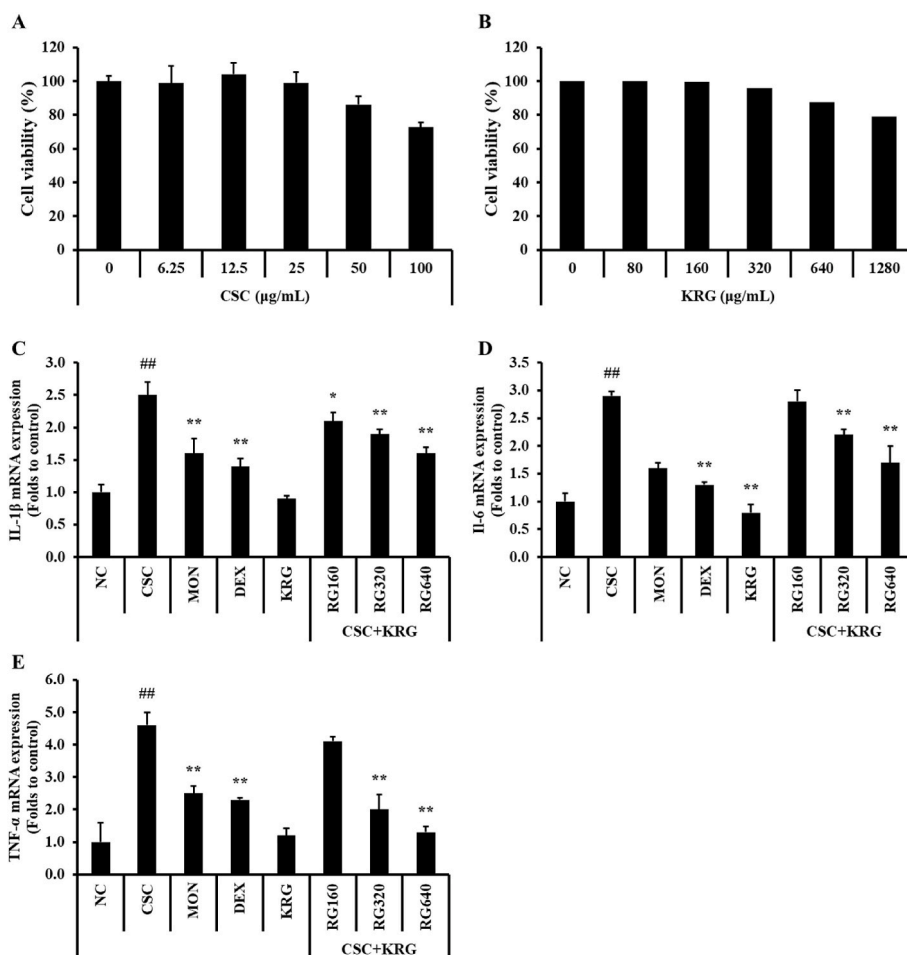
Fig. 4. The doses of (A) cigarette smoke condensate (CSC) and (B) Korean Red Ginseng (KRG) used in the experiments were determined according to the results of cell viability test on NCI–H292 cells. KRG reduces the elevated levels of (C) interleukin (IL)-1β, (D) IL-6, and (E) tumor necrosis factor (TNF)-α in the CSC-stimulated cells. NC; non-treated cells, CSC; stimulation of CSC, MON; stimulation of CSC + treatment of Montelukast sodium 10μM, DEX; stimulation of CSC + treatment of Dexamethasone 1μM, KRG; treatment of 640 μg/mL of KRG; KRG160, 320, and 640; stimulation of CSC + treatment of 160, 320, and 640 μg/mL of KRG. Values: means ± standard deviation ($n = 3$). Significance: $^{##}p < 0.01$ vs NC; *, $**p < 0.05$ and 0.01 vs CSC, respectively.

classified into anti-apoptotic proteins, such as Bcl-2, and pro-apoptotic proteins, such as Bax. A reduction in the Bcl-2/Bax ratio has been shown to induce apoptotic cell death by activating the mitochondrial-dependent Caspase cascade [32]. Many studies have reported an increase in apoptosis during the pathogenesis of emphysema [33,34]. According to several studies, the Bax/Bcl-2 ratio is closely related to the apoptotic mechanism that induces emphysema [35] and Morissette et al [36] reported that the Bax/Bcl ratio was increased in human emphysema. In particular, Zhou et al [37] reported CS-induced emphysema in rats, although the varied Bax and Bcl-2 expression values resulted in apoptosis. In the present study, KRG attenuated the Bax/Bcl-2/Caspase 3 apoptotic signaling induced by CSC treatment, which resulted in emphysema. The effects of KRG were confirmed by TUNEL staining and IHC for Caspase 3. Our results indicate that KRG effectively reduced CSC-induced apoptosis and emphysematous lesions through Bax/Bcl-2/Caspase 3 signaling.

In the present study, KRG significantly reduced CSC-induced VEGF expression followed by PI3K/AKT phosphorylation. VEGF, an important angiogenic growth factor, contributes to nonspecific airway hyper-responsiveness and enhances airway smooth muscle cell proliferation [38]. Numerous studies have demonstrated that the PI3K/AKT pathway is a major downstream pathway of VEGF [39–41]. According to Golpon et al [42], apoptosis induces the expression of growth and survival factors, especially VEGF. Furthermore, higher VEGF expression has been found in the lungs of COPD patients in clinical trials [43]. In particular,

Tsurutani et al [44] found that tobacco components stimulated AKT-dependent proliferation or survival in lung cancer cells. Based on previous studies and our results, CSC-induced apoptosis induces cell survival pathways such as VEGF/PI3K/AKT signaling, while KRG reduces CSC-induced apoptosis, which leads to a decrease in the upregulation of cell survival pathways. However, because several studies have reported that the activation of VEGF/PI3K/AKT signaling inhibits apoptotic changes, further time-course studies or specific protein silencing studies are needed to explain the clear correlation between apoptosis and VEGF/PI3K/AKT signaling [40,45].

The protective effects of KRG are connected to its ginsenosides, including Rb1, Rg1, and Rg3 [46]. Rb1 attenuates pulmonary inflammatory cytokine release and lung tissue injury [47]. Rg1 ameliorates the CS-induced lung epithelial-mesenchymal transition and Rg3 significantly reduces pulmonary fibrosis [15,48]. These results strongly support the protective effects of KRG against pulmonary disease.

Overall, KRG significantly alleviated the emphysematous lesions induced by CSC administration. The protective effects of KRG are closely related to the reduced macrophage population, as well as down-regulation of the apoptotic and cell survival pathways. Our results suggest that KRG could be a potential curative agent for the alleviation of emphysema in COPD patients.
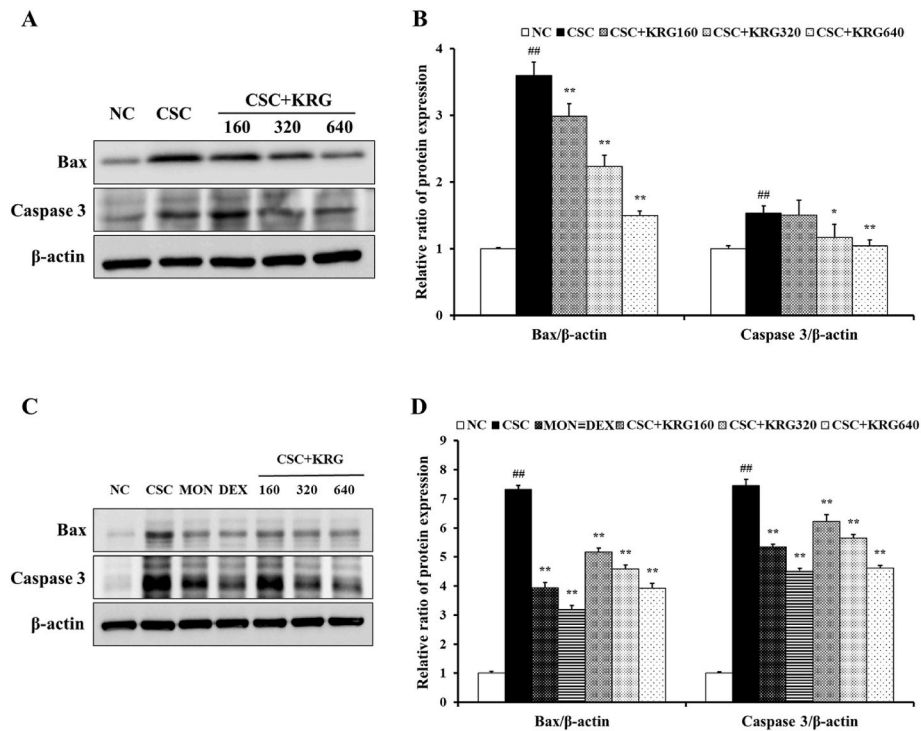
Fig. 5. Korean Red Ginseng (KRG) reduces the elevated expression of (A), (C) Bcl-2-associated X protein (Bax) and Caspase 3 in the CSC-stimulated cells. (B), (D) The densitometric values were determined using Chemi-Doc. NC; non-treated cells, CSC; stimulation of CSC, MON; stimulation of CSC + treatment of Montelukast sodium 10μM, DEX; stimulation of CSC + treatment of Dexamethasone 1μM, KRG; treatment of 640 μg/mL of KRG; KRG160, 320, and 640; stimulation of CSC + treatment of 160, 320, and 640 μg/mL of KRG. Values: means ± standard deviation ($n = 3$). Significance: $^{\#\#}p < 0.01$ vs NC; *, ** $p < 0.05$ and 0.01 vs CSC, respectively.
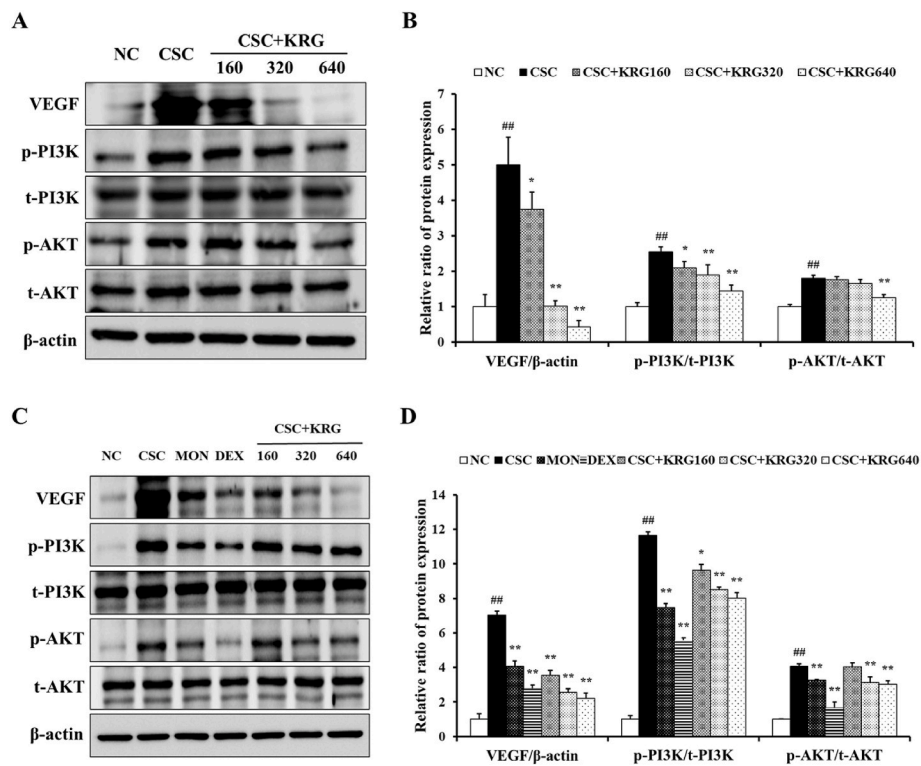
Fig. 6. Korean Red Ginseng (KRG) reduces the elevated expression of (A), (C) vascular endothelial growth factor (VEGF), and phosphorylation of phosphatidyli-nositol 3-kinase (PI3K) and protein kinase B (AKT) in the CSC-stimulated cells. (B), (D) The densitometric values were determined using Chemi-Doc.NC; non-treated cells, CSC; stimulation of CSC, MON; stimulation of CSC + treatment of Montelukast sodium 10μM, DEX; stimulation of CSC + treatment of Dexamethasone 1μM, KRG; treatment of 640 μg/mL of KRG; KRG160, 320, and 640; stimulation of CSC + treatment of 160, 320, and 640 μg/mL of KRG. Values: means ± standard deviation ($n = 3$). Significance: $^{\#\#}p < 0.01$ vs NC; *, ** $p < 0.05$ and 0.01 vs CSC, respectively.

Author contributions

Jeong-Won Kim performed in vivo and in vitro experiments and wrote the manuscript. Jin-Hwa Kim, Chang-Yeop Kim, and Ji-Soo Jeong performed model building and drug treatments. Je-Won Ko and Tae-Won Kim designed the project and wrote the manuscript. All authors discussed and commented on the manuscript.

Declaration of competing interest

The authors declare no conflict of interest.

Acknowledgements

Appendix A. Supplementary data

Supplementary data to this article can be found online at https://doi.org/10.1016/j.jgr.2023.11.001.

References

[1] World Health Organization. The top 10 causes of death. 2019 November. https://www.who.int/en/news-room/fact-sheets/detail/the-top-10-causes-of-death.

[2] Collaborators GBD. Global, regional, and national incidence, prevalence, and years lived with disability for 354 diseases and injuries for 195 countries and territories, 1990-2017: a systematic analysis for the Global Burden of Disease Study 2017. Lancet 2018;392(10159):1789–858.

[3] World Health Organization. COPD management. 2019 December. https://www.who.int/respiratory/copd/management/en/.

[4] Kurashima K, Takaku Y, Ohta C, Takayanagi N, Yanagisawa T, Kanauchi T, Takahashi O. Smoking history and emphysema in asthma-COPD overlap. Int J Chron Obstr Pulmon Dis 2017;12:3523–32.

[5] Goldklang M, Stockley R. Pathophysiology of emphysema and implications. Chronic Obstr Pulm Dis 2016;3(1):454–8.

[6] Gwinn MR, Vallyathan V. Respiratory burst: role in signal transduction in alveolar macrophages. J Toxicol Environ Health B Crit Rev 2006;9(1):27–39.

[7] Grashoff WF, Sont JK, Sterk PJ, Hiemstra PS, de Boer WI, Stolk J, Han J, van Krienken JM. Chronic obstructive pulmonary disease: role of bronchiolar mast cells and macrophages. Am J Pathol 1997;151(6):1785–90.

[8] Di Stefano A, Capelli A, Lusuardi M, Balbo P, Vecchio C, Maestrelli P, Mapp CE, Fabbri LM, Donner CF, Saetta M. Severity of airflow limitation is associated with severity of airway inflammation in smokers. Am J Respir Crit Care Med 1998;158:1277–85.

[9] Choi MK, Song IS. Interactions of ginseng with therapeutic drugs. Arch Pharm Res 2019;42(10):862–78.

[10] In G, Seo HK, Park HW, Jang KH. A metabolomic approach for the discrimination of red ginseng root parts and targeted validation. Molecules 2017;22(3):471.

[11] So SH, Lee JW, Kim YS, Hyun SH, Han CK. Red ginseng monograph. J Ginseng Res 2018;42(4):549–61.

[12] Li J, Lu K, Sun F, Tan S, Zhang X, Sheng W, Hao W, Liu M, Lv W, Han W. Panaxydol attenuates ferroptosis against LPS-induced acute lung injury in mice by Keap1-Nrf2/HO-1 pathway. J Transl Med 2021;19(1):96.

[13] Kim JH, Kim JW, Kim CY, Jeong JS, Lim JO, Ko JW, Kim TW. Korean red ginseng ameliorates allergic asthma through reduction of lung inflammation and oxidation. Antioxidants 2022;11:1422.

[14] Shergis JL, Di YM, Zhang AL, Vlahos R, Helliwell R, Ye JM, Xue CC. Therapeutic potential of Panax ginseng and ginsenosides in the treatment of chronic obstructive pulmonary disease. Complement Ther Med 2014;22(5):944–53.

[15] Guan S, Xu W, Han F, Gu W, Song L, Ye W, Liu Q, Guo X. Ginsenoside Rg1 attenuates cigarette smoke-induced pulmonary epithelial-mesenchymal transition via inhibition of the TGF-β1/smad pathway. Biomed Res Int 2017;2017:7171404.

[16] Kim S, Kim N, Jeong J, Lee S, Kim W, Ko SG, Kim B. Anti-cancer effect of Panax ginseng and its metabolites: from traditional medicine to modern drug discovery. Processes 2021;9:1344.

[17] Lim JO, Kim WI, Lee SJ, Pak SW, Cho YK, Kim JC, Kim JS, Shin IS. The involvement of PDE4 in the protective effects of melatonin on cigarette-smoke-induced chronic obstructive pulmonary disease. Molecules 2021;26(21):6588.

[18] Park SJ, Noh J, Jeong EJ, Kim YS, Han BC, Lee SH, Moon KS. Subchronic oral toxicity study of Korean red ginseng extract in Sprague-Dawley rats with a 4-week recovery period. Regul Toxicol Pharmacol 2018;92:83–93.

[19] Kim CY, Kim JW, Kim JH, Jeong JS, Lim JO, Ko JW, Kim TW. Inner shell of the chestnut (Castanea crenata) suppresses inflammatory responses in ovalbumin-induced allergic asthma mouse model. Nutrients 2022;14:2067.

[20] Hsia CC, Hyde DM, Ochs M, Weibel ER. An official Research policy statement of the American thoracic society/European respiratory society: standards for quantitative assessment of lung structure. Am J Respir Care Med 2010;181(4):394–418.

[21] Ko JW, Shin NR, Jung TY, Shin IS, Moon C, Kim SH, Lee IC, Kim SH, Yun WK, Kim HC, et al. Melatonin attenuates cisplatin-induced acute kidney injury in rats via induction of anti-aging protein. Klotho. Food Chem Toxicol 2019;129:201–10.

[22] Sharafkhaneh A, Hanania NA, Kim V. Pathogenesis of emphysema: from the bench to the bedside. Proc Am Thorac Soc 2008;5(4):475–7.

[23] Akata K, van Eeden SF. Lung macrophage functional properties in chronic obstructive pulmonary disease. Int J Mol Sci 2020;21(3):853.

[24] Shapiro SD. The macrophage in chronic obstructive pulmonary disease. Am J Respir Crit Care Med 1999;160:S29–32.

[25] Vlahos R, Bozinovski S. Role of alveolar macrophages in chronic obstructive pulmonary disease. Front Immunol 2014;5:435.

[26] Miyata R, van Eeden SF. The innate and adaptive immune response induced by alveolar macrophages exposed to ambient particulate matter. Toxicol Appl Pharmacol 2011;257(2):209–26.

[27] Hu G, Dong T, Wang S, Jing H, Chen J. Vitamin D3-vitamin D receptor axis suppresses pulmonary emphysema by maintaining alveolar macrophage homeostasis and function. EBioMedicne 2019;45:563–77.

[28] Pesci A, Balbi B, Cacciani G, Bertacco S, Alciato P, Donner CF. Inflammatory cells and mediators in bronchial lavage of patients with chronic obstructive pulmonary disease. Eur Respir J 1998;12(2):380–6.

[29] Finkelstein R, Fraser RS, Ghezzo H, Cosio MG. Alveolar inflammation and its relation to emphysema in smokers. Am J Respir Crit Care Med 1995;152:1666–72.

[30] Goldsmith CA, Imrich A, Danaee H, Ning YY, Kobzik L. Analysis of air pollution particulate-mediated oxidant stress in alveolar macrophages. J Toxicol Environ Health A 1998;54:529–45.

[31] Martinou JC, Youle RJ. Mitochondria in apoptosis: Bcl-2 family members and mitochondrial dynamics. Dev Cell 2011;21(1):92–101.

[32] Lan CH, Sheng JQ, Fang DC, Meng QZ, Fan LL, Huang ZR. Involvement of VDAC1 and Bcl-2 family of proteins in VacA-induced cytochrome c release and apoptosis of gastric epithelial carcinoma cells. J Dig Dis 2010;11(1):43–9.

[33] Chambers E, Rounds S, Lu Q. Pulmonary endothelial cell apoptosis in emphysema and acute lung injury. Adv Anat Embryol Cell Biol 2018;228:63–86.

[34] Demedts IK, Demoor T, Bracke KR, Joos GF, Brusselle GG. Role of apoptosis in the pathogenesis of COPD and pulmonary emphysema. Respir Res 2006;7(1):53.

[35] Matsuyama S, Palmer J, Bates A, Poventud-Fuentes I, Wong K, Ngo J, Matsutama M. Bax-induced apoptosis shortens the life span of DNA repair defect Ku70-knockout mice by inducing emphysema. Exp Biol Med 2016;241(12):1265–71.

[36] Morissette MC, Vachon-Beaudoin G, Parent J, Chakir J, Milot J. Increased p53 level, Bax/Bcl-x(L) ratio, and TRAIL receptor expression in human emphysema. Am J Respir Crit Care Med 2008;178(3):240–7.

[37] Zhou Y, Tan X, Kuang W, Liu L, Wan L. Erythromycin ameliorates cigarette-smoke-induced emphysema and inflammation in rats. Transl Res 2012;159(6):464–72.

[38] Su X, Taniuchi N, Jin E, Fujiwara M, Zhang L, Ghazizadeh M, Tashimo H, Yamashita N, Ohta K, Kawanami O. Spatial and phenotypic characterization of vascular remodeling in a mouse model of asthma. Pathobiology 2008;75:42–56.

[39] Karar J, Maity A. PI3K/AKT/mTOR pathway in angiogenesis. Front Mol Neurosci 2011;4:51.

[40] Peng N, Gao S, Guo X, Wang G, Cheng C, Li M. Silencing of VEGF inhibits human osteosarcoma angiogenesis and promotes cell apoptosis via VEGF/PI3K/AKT signaling pathway. Am J Transl Res 2016;8:1005–15.

[41] Sun S, Gong F, Liu P, Miao Q. Metformin combined with quercetin synergistically repressed prostate cancer cells via inhibition of VEGF/PI3K/Akt signaling pathway. Gene 2018;664:50–7.

[42] Golpon HA, Fadok VA, Taraseviciene-Stewart L, Scerbavicius R, Sauer C, Welte T, Henson PM, Voelkel NF. Life after corpse engulfment: phagocytosis of apoptotic cells leads to VEGF secretion and cell growth. FASEB J 2004;18(14):1716–8.

[43] Kranenburg AR, de Boer WI, Alagappan VK, Sterk PJ, Sharma HS. Enhanced bronchial expression of vascular endothelial growth factor and receptors (Flk-1 and Flt-1) in patients with chronic obstructive pulmonary disease. Thorax 2005;60:106–13.

[44] Tsurutani J, Castillo SS, Brognard J, Granville CA, Zhang C, Gills JJ, Sayyah J, Dennis PA. Tobacco components stimulate Akt-dependent proliferation and NFkappaB-dependent survival in lung cancer cells. Carcinogenesis 2005;26(7):1182–95.

[45] Wen N, Guo B, Zheng H, Xu L, Liang H, Wang Q, Wang D, Chen X, Zhang S, Li Y, et al. Bromodomain inhibitor jq1 induces cell cycle arrest and apoptosis of glioma stem cells through the VEGF/PI3K/AKT signaling pathway. Int J Oncol 2019;55(4):879–95.

[46] Kim JH, Yi YS, Kim MY, Cho JY. Role of ginsenosides, the main active components of Panax ginseng, in inflammatory responses and diseases. J Ginseng Res 2017;41(4):435–43.

[47] Jiang Y, Zhou Z, Meng QT, Sun Q, Su W, Lei S, Xia Z, Xia ZY. Ginsenoside Rb1 treatment attenuates pulmonary inflammatory cytokine release and tissue injury following intestinal ischemia reperfusion injury in mice. Oxid Med Cell Longev 2015;2015:843721.

[48] Fu Z, Xu YS, Cai CQ. Ginsenoside Rg3 inhibits pulmonary fibrosis by preventing HIF-1α nuclear localisation. BMC Pulm Med 2021;21(1):70.